Arch. Min. Sci. **70** (2025), 4, 643-656

Electronic version (in color) of this paper is available: http://mining.archives.pl

DOI: https://doi.org/10.24425/ams.2025.157452

HAILONG MU[1], SHENGJUN ZHANG[2*]

STUDY ON PROPAGATION ATTENUATION LAW OF VIBRATION WAVE IN COAL ROCK

The disturbance of vibration wave will have a great influence on the internal stress, pore fissure and gas adsorption of coal and rock mass. The typical earthquake and mine earthquake waveform records in the mining area are selected. Combined with the comprehensive histogram of the working face, the calculation model is established by UDEC software, and the propagation attenuation law of vibration wave in the presence or absence of chamber is analyzed. The calculation results show that: (1) Under the condition of no chamber, the peak velocity of seismic wave decreases exponentially with the increase of source distance, and the fitting accuracy R^2 of seismic wave and mine seismic wave attenuation characteristics is 0.96 and 0.98 respectively. (2) The peak velocity of seismic wave decreases exponentially with the increase of focal distance under the condition of chamber. However, there is a transition point at the chamber (goaf), which attenuates at a faster speed before passing through the chamber, and the attenuation speed slows down after passing through the chamber. The attenuation rate of the peak velocity of the earthquake and the mine earthquake reached 53.9% and 46.8% respectively when passing through the chamber. (3) The peak velocity of the vibration wave is the largest at the left/right foot of the chamber, and the peak velocity of the vault is the smallest. (4) The velocity attenuation curve of the source ring of the seismic wave decreases faster in the vertical direction than in the horizontal direction, and the attenuation in the vertical direction is particularly obvious after passing through the chamber. The propagation and attenuation characteristics of vibration waves are of great significance to the prevention and control of rock burst in coal mines, the development characteristics of coal and rock pores and fractures, and the early warning of gas disasters.

Keywords: Vibration wave; chamber; attenuation law; peak velocity; the source ring

[1] NINGXIA TRANSPORTATION SCIENCE RESEARCH INSTITUTE CO., LTD; INSTITUTE OF ENGINEERING MECHANICS, CHINA EARTHQUAKE ADMINISTRATION, CHINA

[2] NINGXIA ACADEMY OF AGRICULTURE AND FORESTRY SCIENCES, CHINA

* Corresponding author: shengjun812@163.com

© 2025. The Author(s). This is an open-access article distributed under the terms of the Creative Commons Attribution License (CC-BY 4.0). The Journal license is: https://creativecommons.org/licenses/by/4.0/deed.en. This license allows others to distribute, remix, modify, and build upon the author's work, even commercially, as long as the original work is attributed to the author.

1. Introduction

Based on the characteristics of China's resource endowment, the structure of coal as the main energy consumption in China will not change in the short term [1,2]. Stable coal supply and disaster prevention and control technology are strategic needs for a long time in the future. At present, China 's coal mining has entered the stage of deep mining. The coal and gas occurrence environment is extremely complex. Under the disturbance of vibration waves, it is easy to induce dynamic disasters such as rock burst, coal and gas outburst and surface subsidence [3-7]. Through research and statistics, it is found that not only frequent mine earthquakes, but also natural earthquakes and artificial blasting often occur in the mining area [8-10]. The disturbance of vibration wave will have a great influence on the internal stress, pore fissure and gas adsorption state of coal rock mass. Therefore, it is of great significance to study the propagation and attenuation law of vibration wave in coal rock to understand the stress of coal seam and the development of pore cracks, and to intervene and warn the disaster in advance.

A large number of joints and other discontinuities in coal and rock mass significantly affect the mechanical properties of rock mass, and also greatly affect the propagation and attenuation law of stress wave in coal and rock mass [11]. The commonly used numerical simulation methods include finite element method, boundary element method, discontinuous element method and discrete element method. Because coal rock contains natural joints, there are many discontinuities. Therefore, the discrete element method is widely used in the study of stress wave propagation in jointed rock mass [12,13]. The stress response of coal and rock mass caused by earthquake wave propagation and the mechanism of earthquake wave propagation in discontinuous surface can accurately and effectively simulate the attenuation of wave propagation [14,15]. Based on the constructed UDEC-DM model, [16] studied the process of crack initiation, expansion and coalescence in the process of deformation and failure of rock slope. Based on UDEC, [17] simulated the propagation law of explosion stress wave and the expansion process of coal blasting damage zone, and found that the explosion stress wave in coal body decayed nonlinearly and exponentially with the expansion of radial cracks. The attenuation law of explosive stress waves in rock mass obtained by [18,19] through numerical simulation is basically consistent with the theoretical formula calculation results. [20,21] reproduced the propagation process of vibration wave in jointed rock mass by UDEC numerical simulation, and found that the propagation of vibration wave was affected by many factors. The discontinuity surface in coal and rock mass had obvious effect on the propagation of vibration wave, and the discontinuity of medium blocked the stress propagation of vibration wave. [22] analyzed the propagation mode, attenuation characteristics and dynamic stress drop of vibration wave energy excited by mine earthquake. [23] established a simplified model of the stope through UDEC, considering the penetration of joints in practical engineering and the reduction effect of fracture fillers on the strength of structural planes. The distribution of fractures under the coupling of seepage, the influence of seepage on slope stability, the deformation law and failure mechanism inside the slope are analyzed mainly through displacement field, seepage field and stress field.

The initial stress and distribution of different coal and rock mass are different, and the mechanical properties and engineering phenomena are also different under the dynamic action of vibration wave disturbance. In order to control the dynamic disaster caused by dynamic load in deep coal and rock mining engineering, the propagation law of vibration wave is an important

basis for revealing the dynamic disaster induced by mining dynamic load [24]. Based on the engineering background of a mine in Hegang, Heilongjiang Province, this paper selects typical earthquake waves and mine earthquake waves, uses UDEC numerical software to simulate the propagation and attenuation law of earthquake waves in jointed rock mass, analyzes the propagation and attenuation law of stress waves in solid coal area and goaf, and reveals the mechanism of discontinuous surface stress propagation of earthquake waves. It provides theoretical and practical support for the stability analysis and evaluation of coal rock under the vibration wave disturbance of deep coal rock mass.

2. Engineering background

A coal mine in Hegang is located on the northwest side of the Jiayi graben in Heilongjiang Province. It is an east-dipping monoclinic structure with a north-south dip angle of 20°-50°. The strike of the coal-bearing strata is from north to east, and the dip angle of the east-inclined monoclinic structure is generally 30°, with undulating along the local area. The main type of coal rock in the coal seam is semi-quantum rock, followed by dim type, with obvious thin layer of carbon. The structure of coal is complex, with banded and linear structure, brittle structure and developed endogenous cracks. The main coal seam of the working face is 22# coal seam, with an average thickness of 10.15 m. The comprehensive histogram is shown in Fig. 1.

North three four area comprehensive histogram

Lithology	Columnar	Thickness/m	Lithologic description
sandstone-mudstone		36.80	Gray to grayish white, partially interbedded with siltstone, with wavy bedding, containing a small amount of carbonized plant debris.
medium sandstone		16.90	It is grayish white, mainly quartz feldspar, containing a small amount of dark sulfone 0.2-0.5 cm fine particles.
21# coal seam		5.16	Black, mainly massive semi-bright coal.
fine sandstone		2.94	Light gray, mainly quartz feldspar.
21# coal seam		10.15	Black, mainly hard massive semi-bright coal, with dark coal bands.
mudstone		4.42	It is dominated by hydromica and kaolinite, and the bedding is not obvious or massive.
fine sandstone		3.63	White gray-light gray, mainly quartz feldspar, grain average.

Fig. 1. Comprehensive histogram of working face

3. Establishment of the model

3.1. Coal rock mechanical parameters

The physical and mechanical parameters of the overburden strata simulation calculation of the mining face in the north three or four area of the mine are shown in TABLE 1 and TABLE 2.

TABLE 1

Rock mechanics parameters

Rock soil layer class	Density /Kg.m^{-3}	Angle of internal friction/°	Cohesion /MPa	Tensile strength /MPa	Single axis compressive strength/MPa	Elastic modulus /GPa	Poisson ratio
Sand mudstone	2.610	36.0	7.54	4.575	74.900	18.70	0.26
Medium sandstone	2.519	34.0	8.00	4.406	75.231	10.155	0.14
21# coal seam	1.390	25.2	0.87	1.96	8.198	8.62	0.22
Fine sandstone	2.619	35.4	13.20	2.184	51.543	8.251	0.23
22# coal seam	1.459	27.0	0.96	2.01	10.390	8.850	0.24
Mudstone	2.570	34.2	3.41	2.61	72.35	10.750	0.28
Fine sandstone	2.494	35.4	13.20	4.566	106.473	8.661	0.23

TABLE 2

Mechanical parameters of rock joint

Rock soil layer class	Normal stiffness /GPa	Tangential stiffness /GPa	Angle of internal friction/°	Cohesion /MPa	Tensile strength /MPa
Sand mudstone	7.0	7.1	23	1.2	0
Medium sandstone	8.2	8.1	30	1.6	0
Coal seam	5.5	5.9	25	0	0
Mudstone	6.6	7.1	15	0	0
Fine sandstone	8.4	8.1	30	1.5	0

3.2. Establishment of the model

UDEC numerical simulation is an effective method specially used to solve discontinuous media problems. It mainly simulates the mechanical characteristics of discontinuous media such as joints and fissures in rock mass under static or dynamic loads. As a boundary condition, the joint allows the block to move and rotate on the discontinuous surface, and the block can be rigid or deformable. In this paper, the model stratum is simplified into a horizontal model, and a model with a strike of 90 m long and 80 m high is established. The Mohr-Coulomb surface contact slip model is used as shown in formula (1) [25].

$$R = C \cdot \cos\phi + \frac{1}{2}\left(\sigma_1 + \sigma_3\right) \cdot \sin\phi \tag{1}$$

Where: φ is the internal friction angle of rock mass; c is the cohesion of rock mass; σ_1 is the maximum principal stress; σ_3 is the minimum principal stress; r is the radius of stress circle, $R = (\sigma_1\text{-}\sigma_3)/2$.

The left and right boundary of the model is the deformation constraint boundary. The displacement in the *x* direction is defined as 0, the lower boundary is the fixed boundary, the displacement in the *x* and *y* directions is 0, and the upper boundary is the free boundary. The stratum between the upper boundary and the surface of the model is transformed into a vertical uniform load and applied to the upper boundary. The gravity acceleration g is 9.8 m/s^2, and the model diagram is shown in Fig. 2.

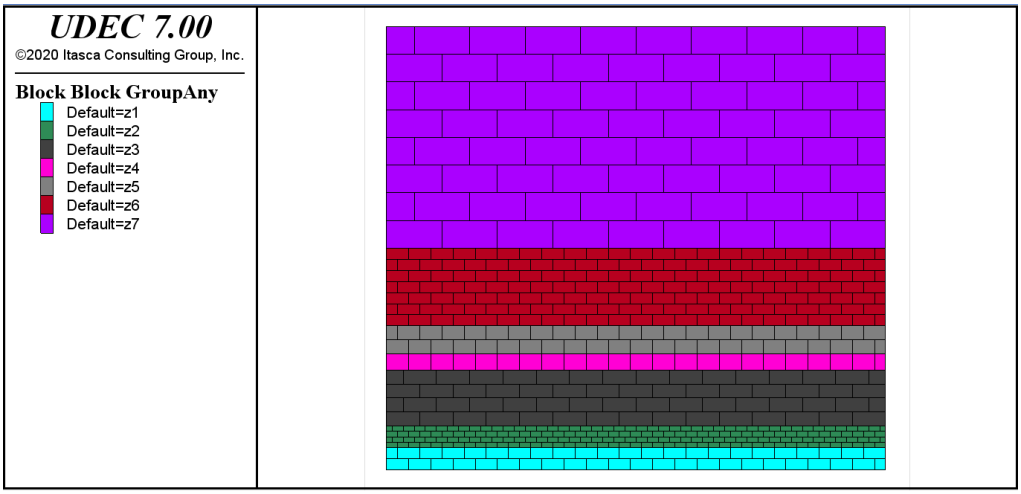

Fig. 2. Construction model

3.3. Monitoring point layout and vibration wave input scheme

Based on the computational model, the initial ground stress balance is calculated by assigning the corresponding mechanical parameters and model constraints to each stratum and contact surface. The monitoring points are placed at each stratigraphic level and at the chamber envelope, and at the source of the earthquake, as shown in Fig. 3. The propagation attenuation law in horizontal and vertical directions can be calculated with or without chamber. The earthquake and mine earthquake velocity time history curves are selected as the input vibration waveforms, which are input from the bottom of the model. The selection of seismic waves comes from the measured records of Hegang Seismic Station. The basic parameters of Hegang Seismic Station are shown in TABLE 3, and the selected seismic records are shown in TABLE 4.

TABLE 3

Instrument Model and Parameters of Hegang Seismic Station

Station name	Station code	Station bedrock	Seismometer type	Data acquisition type	Observation frequency band	Sampling frequency
Hegang station	HEG	granite	CTS-1	EDAS-24L6	50 Hz – 120s	100

TABLE 4

Selected typical mine earthquake, earthquake and blasting records

No	Earthquake time	Longitude	Latitude	Focal depth /km	Magnitude /ML	Epicentral location	Event type
1	2019-01-17 20:14:13	129.79	48.05	8	2.5	Hegang City	earthquake
2	2020-02-26 12:08:43	130.27	47.25	—	2.8	Hegang City	mine earthquake

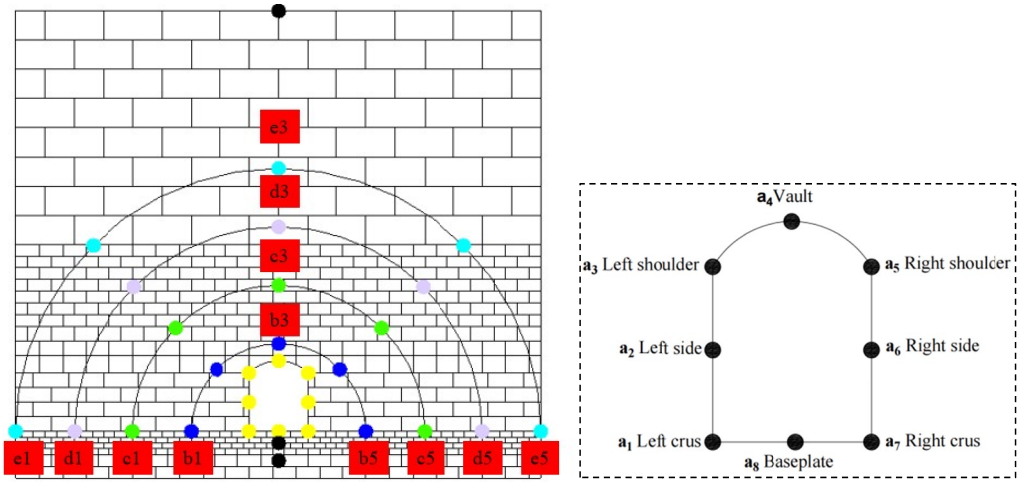

Fig. 3. Monitoring point layout and vibration wave input diagram

4. The propagation attenuation law of vibration wave

4.1. Velocity attenuation characteristics of coal rock without chamber

4.1.1. Earthquake waveform attenuation characteristics

Based on the measured earthquake waveform records, the velocity time history curve is input at the bottom of the model to monitor the velocity attenuation characteristics of different positions of coal rock. The velocity time history curves under different source distances are shown in Fig. 4. we can lear from the figure that the velocity time history curve propagates and attenuates when passing through different coal and rock masses. With the increase of focal distance, the velocity amplitude gradually decreases.

Fig. 5 shows the attenuation characteristics of seismic peak velocity (PGV) in the vertical direction at different source distances. It can be seen from the diagram that the peak velocity decreases exponentially with the increase of the focal distance, and the fitting accuracy R^2 reaches 0.96. This is consistent with the characteristic that Du Taotao's vibration energy decays exponentially with the source distance [26].

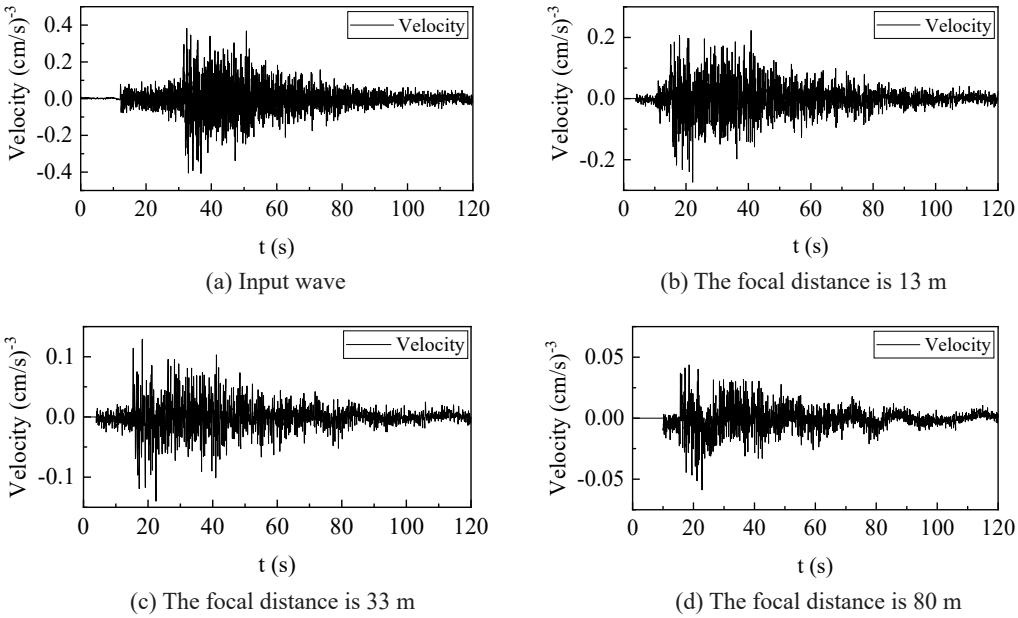

Fig. 4. Attenuation characteristics of earthquake waveform with focal distance

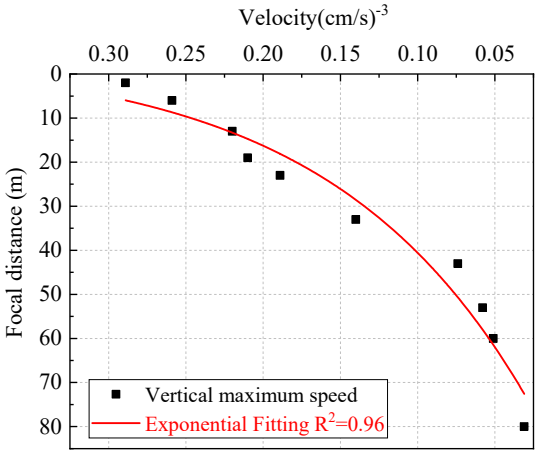

Fig. 5. The attenuation curve of earthquake peak velocity with focal distance

4.1.2. Waveform attenuation characteristics of mine earthquake

The time history curve of mine earthquake velocity under different focal distances is shown in Fig. 6. We can know the propagation attenuation of different coal and rock masses is consistent with the characteristics of earthquake waveform attenuation from this figure. With the increase

of source distance, the velocity amplitude gradually decreases, but the characteristics of velocity time history curve are basically consistent.

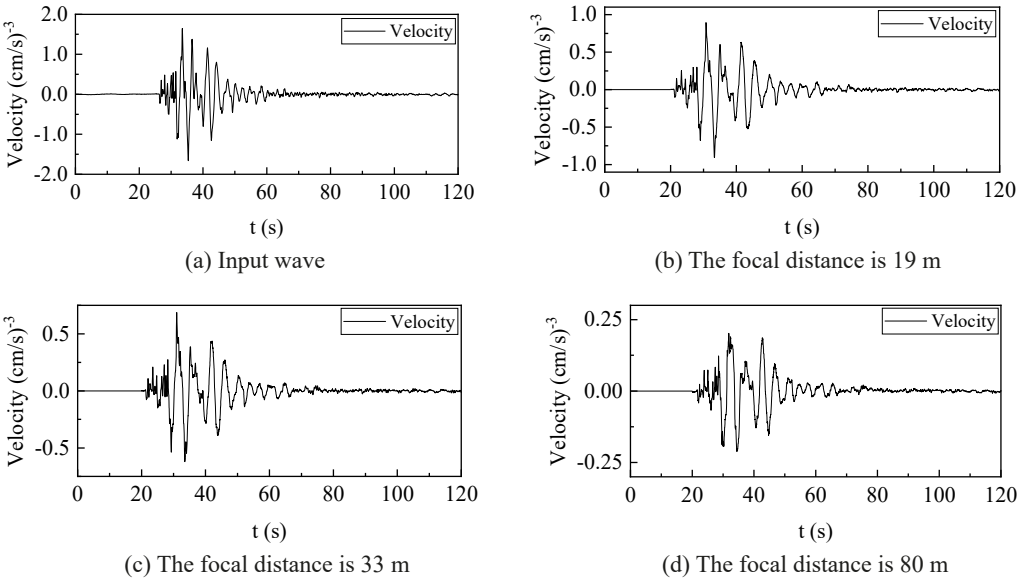

Fig. 6. Attenuation characteristics of mine earthquake waveform with focal distance

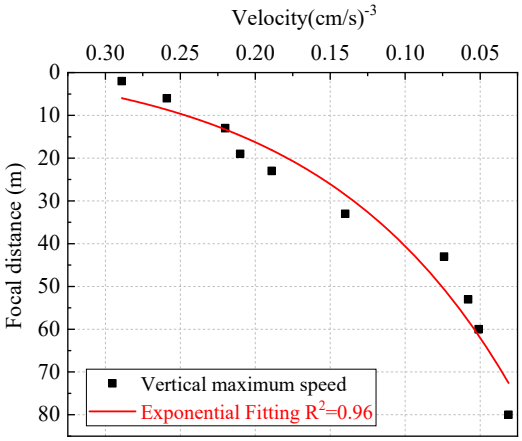

Fig. 7. The attenuation curve of peak velocity of mine earthquake with focal distance

Fig. 7 shows the attenuation characteristics of the peak velocity (PGV) of the vertical mine earthquake under different focal distances. It can be seen from the figure that the peak velocity gradually decreases with the increase of the focal distance, and the peak velocity of the whole process decays rapidly, and it decays exponentially, and the fitting accuracy R^2 reaches 0.98.

4.2. Velocity attenuation characteristics of coal rock with chamber

4.2.1. Earthquake waveform attenuation characteristics

The velocity time history curves of different source distances under the condition of chamber are shown in Fig. 8. From the diagram, which can be show from the figure that after the propagation attenuation of different coal and rock masses, the velocity amplitude gradually decreases with the increase of focal distance, but the time history curve characteristics are basically consistent.

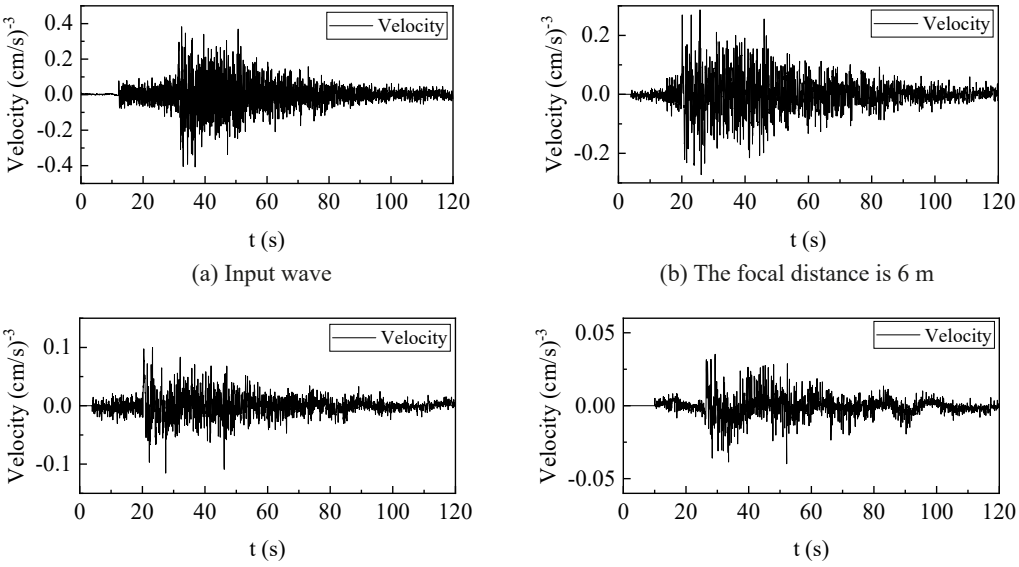

Fig. 8. Attenuation characteristics of earthquake waveform with focal distance

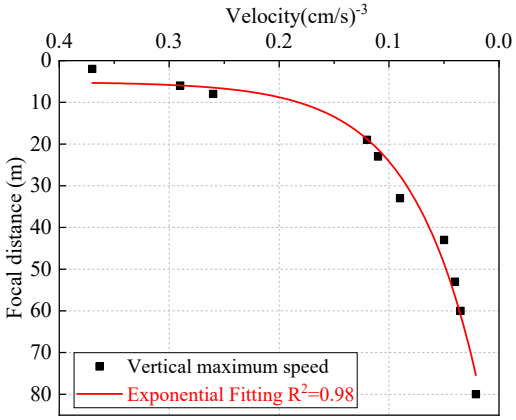

Fig. 9. Attenuation curve of earthquake peak velocity with focal distance

Fig. 9 shows the attenuation characteristics of seismic peak velocity (PGV) at different source distances under the condition of chamber. From the diagram, it can be seen that the peak velocity decreases exponentially with the increase of focal distance, and the fitting accuracy R^2 reaches 0.98. However, it attenuates at a faster rate before passing through the chamber, and the attenuation rate slows down after passing through the chamber. The peak velocity attenuation rate is 53.9% when passing through the chamber (goaf).

4.2.2. Waveform attenuation characteristics of mine earthquake

The velocity time history curves of different source distances under the condition of chamber are shown in (Fig. 10). From the diagram, which can be show from the figure that after the propagation attenuation of different coal and rock masses, the velocity amplitude gradually decreases with the increase of focal distance.

Fig. 11 shows the attenuation characteristics of the peak velocity (PGV) of the mine earthquake under different focal distances under the condition of the chamber. From the figure, it can be seen that the peak velocity gradually decreases with the increase of the focal distance, and the attenuation characteristics and the earthquake are consistent with the exponential function attenuation, and the fitting accuracy R^2 is 0.99. The peak velocity attenuation rate reaches 46.8% when passing through the chamber (goaf).

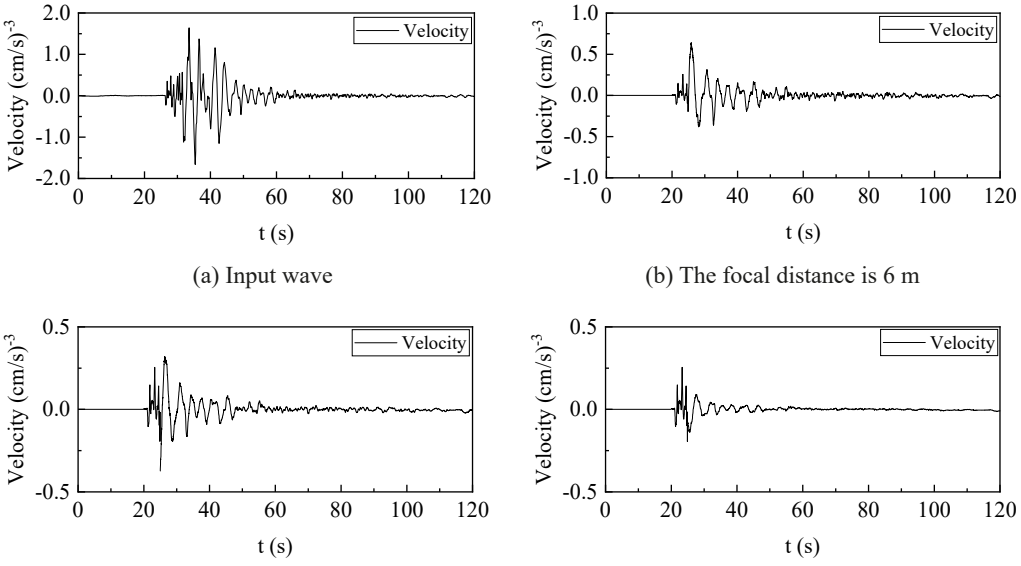

Fig. 10. Attenuation curve of mine earthquake peak velocity with focal distance

4.3. Velocity attenuation law of chamber surrounding rock

The peak velocity of different positions of the surrounding rock under the action of earthquake and mine earthquake wave is shown in Fig. 12. We can know the earthquake and mine

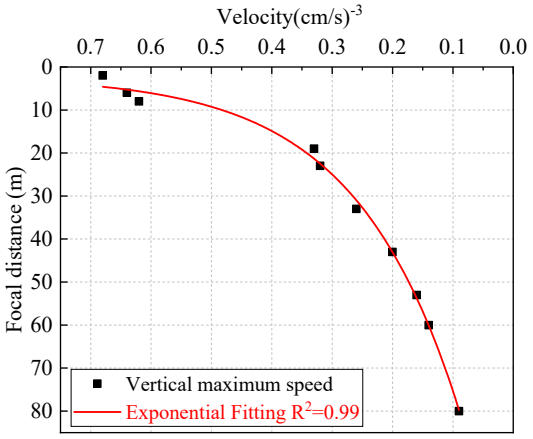

Fig. 11. Attenuation curve of peak velocity of mine earthquake with source distance

earthquake waveforms have consistent propagation attenuation characteristics at the surrounding rock of the chamber from this figure. The peak velocity of the left and right feet of the chamber is the largest, and the attenuation of the vibration wave is the weakest. The peak velocity of the vault is the smallest, indicating that the vibration wave has the fastest attenuation through the goaf.

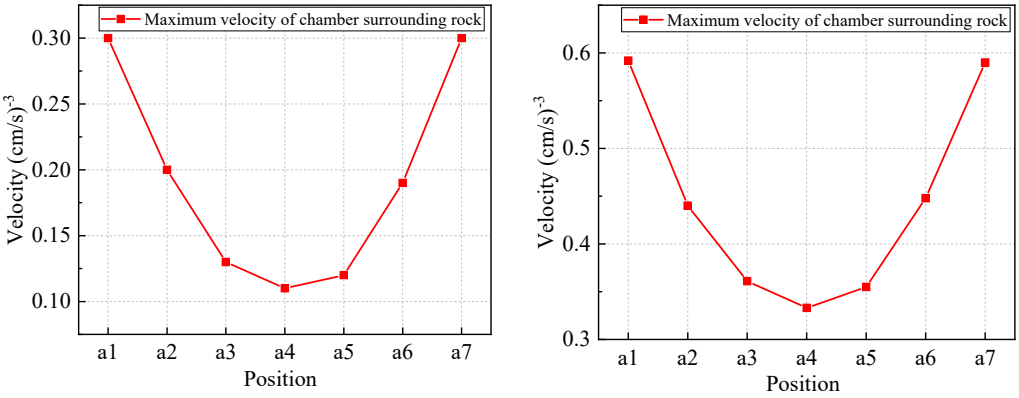

(a) earthquake (b) mine earthquake

Fig. 12. Peak velocity of surrounding rock of chamber

4.4 Velocity attenuation law of focal circle

The velocity attenuation characteristic curve of earthquake source circle under different focal distances is shown in Fig. 13. Which can be shown from the figure that the velocity waveform is larger than the horizontal peak velocity in the vertical direction. The analysis shows that the joint discontinuity surface of different rock strata in the vertical direction leads to the rapid attenuation of the vertical velocity, and the vertical attenuation is particularly obvious after passing through the chamber (goaf).

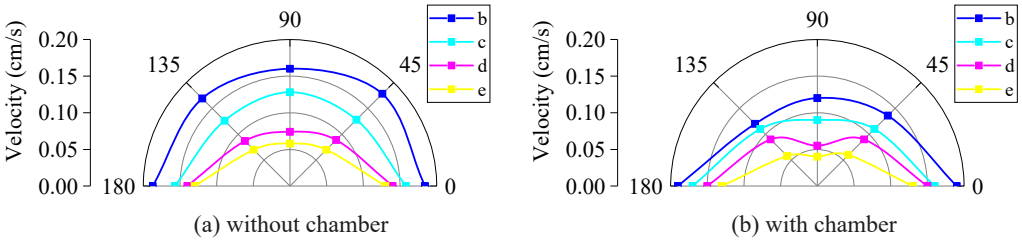

(a) without chamber (b) with chamber

Fig. 13. Earthquake focal circle velocity attenuation curve

The velocity attenuation characteristic curve of mine earthquake source circle under different source distances is shown in Fig. 14. As is shown from figure, the attenuation characteristics of velocity waveform are consistent with those of earthquake, but the propagation attenuation amplitude is larger than that of earthquake.

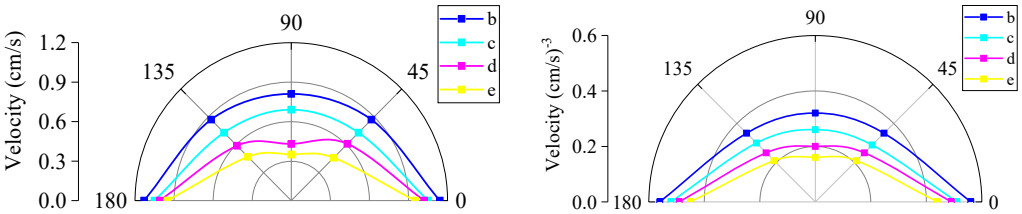

(a) without chamber (b) with chamber

Fig. 14. Mine earthquake focal circle velocity attenuation curve

5. Conclusions

Based on the waveform of earthquake and mine earthquake velocity in mining area, the numerical model of working face is established by using UDEC numerical software. By inputting the time history records of earthquake and mine earthquake velocity, the propagation attenuation law of vibration wave under the condition of chamber or not is analyzed. The specific conclusions are as follows:

(1) Based on the comprehensive histogram of the working face in the mining area and the mechanical parameters of the coal and rock strata, the calculation model was established using UDEC software. Considering the presence or absence of chamber conditions, the monitoring points of the model in the vertical direction of each rock stratum, the source ring and the surrounding rock of the chamber were determined.

(2) The peak velocity propagation attenuation characteristics of seismic wave and mine seismic wave under the condition of no chamber are exponential function attenuation. The fitting accuracy R^2 of seismic wave attenuation characteristics is 0.96, and the fitting accuracy R^2 of mine seismic wave attenuation is 0.98.

(3) The peak velocity attenuation of seismic wave and mine earthquake wave under the condition of chamber is exponential function attenuation, and the fitting accuracy R^2

is 0.98 and 0.99 respectively. However, there is a transition point at the chamber (goaf), which attenuates at a faster speed before passing through the chamber, and the attenuation speed slows down after passing through the chamber. The attenuation rate of the peak velocity of the earthquake and the mine earthquake reached 53.9% and 46.8% respectively when passing through the chamber.

(4) The peak velocity of the left/right foot of the chamber is the largest, and the attenuation of the vibration wave is the weakest. The peak velocity of the vault is the smallest, indicating that the velocity attenuation of the vibration wave through the chamber (goaf) is the fastest.

(5) The velocity attenuation curves of the earthquake and the mine earthquake velocity waveforms under different focal distances are consistent. The peak velocity in the vertical direction is larger than that in the horizontal direction, and the attenuation in the vertical direction is particularly obvious after passing through the chamber.

References

[1] F.M. Li, Current Status and Developm ent Tendency of CoalM in ing Subsidence A rea Treatment Technology in China. Journal of Mining and Strata Control Engineering **16** (3), 8-10(2011).

[2] Z.X. Jin, M.T. Cao, H.W. Wang, New opportunities for coal industry transformation and development under the background of the level of a moderately developed country and a new “dual control” system. Coal Science and Technology **51** (01), 45-58 (2023).

[3] L. Wojtecki, P. Konicek, J. Schreiber, Effects of torpedo blasting on rockburst prevention during deep coal seam mining in the Upper Silesian Coal Basin. Journal of Rock Mechanics and Geotechnical Engineering **9** (04), 694-701 (2017). DOI: https://doi.org/10.1016/j.jrmge.2017.03.014

[4] L. Yuan, Research progress on risk identification, assessment, monitoring and early warning technologies of typical dynamic hazards in coal mines. Journal of China Coal Society **45** (05), 1557-1566 (2020).

[5] L.M. Dou, Z.L. Mou, AY. Cao, Coal mine rock burst prevention and control, 2017 Science Press, Beijing.

[6] Q.X. Qi, Y.Z. Li, S.K. Zhao, N.B. Zhang, W.Y. Zheng, H.T. Li, H.Y. Li, Seventy years development of coal mine rockburst in China: establishment and consideration of theory and technology system. Coal Science and Technology **47** (09), 1-40 (2019).

[7] L. Chen, L. Yu, J. Ou, Y.B. Zhou, F. Wang, Prediction of coal and gas outburst risk at driving working face based on Bayes discriminant analysis model. Earthquakes and Structures **18** (1), 73-82 (2020). DOI: https://doi.org/10.12989/eas.2020.18.1.073

[8] S.J. Meng, W.H. Yang, H.Y. Li, M. Wang, Y.Q. Sun, Preliminary study on the early warning of coal mine gas disaster induced by shake. World Earthquake Engineering **36** (02), 218-228 (2020).

[9] S.J. Meng, H.L. Mu, M. Wang, W.H. Yang, Y. Liu, Y. Q. Sun, X.M. Yuan, Characteristics and Identification Method of Natural and Mine Earthquakes: A Case Study on the Hegang Mining Area. Minerals **12**, 1256 (2022). DOI: https://doi.org/10.3390/min12101256

[10] W.H. Yang, Research on Recognition Method of Earthquake and Mine Earthquake Based on Hegang Area. Master, thesis. Harbin University of Science and Technology, 2020.

[11] S.B. Chai, J.H. Zhao, H. Wang, UDEC simulation on cylindrical wave propagation through jointed rock masses. Chinese Journal of Rock Mechanics and Engineering **38** (S1), 2848-2856 (2019).

[12] X.B. Zhao, J. Zhao, J.G. Cai, A.M. Hefny, UDEC modeling on wave propagation across fractured rock masses. Computers and Geotechnics **35** (1), 97-104 (2008). DOI: https://doi.org/10.1016/j.compgeo.2007.01.001

[13] H. Dadkhah, M. Mohebbi, A multi-hazard-based design approach for LRB isolation system against explosion and earthquake. Earthquake and Structures **21** (1), 95-111 (2021).

[14] F.Q. Gao, D. Stead, The application of a modified Voronoi logic to brittle fracture modelling at the laboratory and field scale-ScienceDirect,. International Journal of Rock Mechanics and Mining Sciences **68**, 1-14 (2014). DOI: https://doi.org/10.1016/j.ijrmms.2014.02.003

[15] X.F. Deng, J.B. Zhu, S.G. Chen, Z.Y. Zhao, Y.X. Zhou, J. Zhao, Numerical study on tunnel damage subject to blast-induced shock wave in jointed rock masses, Tunnelling and Underground Space Technology **43**, 88-100(2014). DOI: https://doi.org/10.1016/j.tust.2014.04.004

[16] H.J. Liu, X.W. Hu, J.J. Chen, F.K. Ni, Rearch on deformation and rupture evolution process of rock slope based on UDEC-DM method. Low Temperature Architecture Technology **40** (12), 100-104 (2018).

[17] F. Xie, P. Cao, Y.L. Hao, Numerical Simulation of Deep-hole Presplitting Blasting in Coal Seam by UDEC Modeling. Blasting **33** (01), 73-77 (2016).

[18] P. Cao, S.L. Yan, L. Ni, F. Liu, Y.J. Li, Research on Attenuation Law of Explosion Stress Wave in Rock by UDEC Modeling. Blasting **31** (01), 42-46 (2014).

[19] W.Z. Chen, X.Q. Liu, B. Li, Numerical Simulation of Stress Wave Attenuation of Rock. Journal of University of South China (Science and Technology) **30** (01), 118-123 (2016).

[20] L.M. Dou, J.R. Cao, A.Y. Cao, Y.J. Chai, J.Z Bai, J.L. Kan, Research on types of coal mine tremor and propagation law of shock waves. Coal Science and Technology **49** (06), 23-31 (2021).

[21] G.A. Zhu, Q.P. Jiang, Y.P. Wu, L.M. Dou, Z.Q. Lin, H.Y. Liu, Numerical inversion of dynamic behavior of fault slip instability induced by stress waves. Journal of Mining and Safety Engineering **38** (02), 370-379 (2021).

[22] A.Y. Cao, J. Fan, Z.L. Mou, X.Q. Guo, Burst failure effect of mining-induced tremor on roadway surrounding rock,. Journal of China Coal Society **35** (12), 2006-2010 (2010).

[23] L. Pan, The Seepage Analysis of Fractured Rock Mass Based on UDEC. Master, thesis. University of Science and Technology Liaoning, Anshan, 2016.

[24] J. He, Research of Mining Dynamic Loading Effect and Its Induced Rock Burst in Coal Mine. Ph.D, thesis. China University of Mining and Technology, Xuzhou, 2013.

[25] H.J. Liao, Numerical analysis for geotechnical engineering structure. 2009 China Machine Press, Beijing.

[26] T.T. Du, Propagation and response laws of mine seism. Chinese Journal of Geotechnical Engineering **40** (03), 418-425 (2018).